ELSEVIER

PII: S0032-3861(96)00725-2

Polymer Vol. 38 No. 8, pp. 1779–1785, 1997

0032-3861/97/$17.00 + 0.00

Microphase domains of poly(styrene-*block*-ethylene/butylene-*block*-styrene) triblock copolymers studied by atomic force microscopy

Makoto Motomatsu*
Joint Research Center for Atom Technology (JRCAT), Angstrom Technology Partnership (ATP), 1-1-4 Higashi, Tsukuba, Ibaraki 305, Japan

and Wataru Mizutani† and Hiroshi Tokumoto†
Joint Research Center for Atom Technology (JRCAT), National Institute for Advanced Interdisciplinary Research (NAIR), 1-1-4 Higashi, Tsukuba, Ibaraki 305, Japan
(Received 23 April 1996; revised 6 June 1996)

Atomic force microscopy has been successfully used to observe morphologies and characterize polymer components of poly(styrene-*block*-ethylene/butylene-*block*-styrene) (SEBS) triblock copolymer surfaces. The surfaces exhibited characteristic topographies consisting of hills and valleys. The height difference between them increased with the polystyrene component, which is probably due to the stress increase between two phases. The surface area fraction of the hills also increased with polystyrene component, and the local stiffness of the hills was higher than that of the valleys. These results indicate that the hills correspond to polystyrene and the valleys to rubbery poly(ethylene/butylene). The morphology of polystyrene changed from long worm-like to mesh-like structures with increasing polystyrene content in the block copolymers and exhibited a moniliform-like structure with a periodicity of 20–30 nm. These structures may be caused by surface segregation of the polystyrene component in the block copolymer surface.

(Keywords: atomic force microscopy; SEBS; surface segregation)

INTRODUCTION

Organic polymers exhibit a variety of material properties. For example, Young's modulus ranges from 10^5 Pa for rubbers to 5×10^9 Pa for rigid polymers[1]. Such a wide range can be realized by changing the molecular weight, the blend ratio and the component ratio not only in simple homopolymers but also in polymer hybrids such as physical blends and copolymers. We can therefore design materials with new and unusual properties in these systems. Among them, block copolymer systems consisting of chemically different and terminally connected segments are widely used for interface adhesives, compatilizers and surface modifiers by physical entanglement and entrapment[2]. They usually exhibit phase separation on a micrometre scale down to a nanometre scale[3].

Nanometre-scale bulk properties of such polymers have been mainly studied using either transmission electron microscopy (TEM)[4,5] or small-angle X-ray scattering (SAXS)[6,7]. Although the study of the surface properties of these polymers is important in order to understand the surface segregation and polymer–air interface effects which determine wettability, adhesion etc., few reports have focused on this subject. Recently, atomic force microscopy (AFM)[8] has opened a new world for investigating polymer surfaces on a nanometre scale[9–15]. Various force microscopy techniques[16,17] enable us to measure local mechanical properties such as friction and stiffness which are specific to individual polymers[18–20].

By using AFM techniques, we have investigated microstructures and microphase separations in air, which are influenced by surface segregation. In this paper we shall show systematic results for individual polymers of thermoplastic triblock copolymers composed of a hard segment of polystyrene and a soft segment of poly(ethylene/butylene), poly(styrene-*block*-ethylene/ butylene-*block*-styrene), with different weight ratios of the polystyrene component.

EXPERIMENTAL

Three types of poly(styrene-*block*-ethylene/butylene-*block*-styrene) (SEBS) material were synthesized by hydrogenating anionically polymerized poly(styrene-*block*-butadiene-*block*-styrene) triblock copolymers‡. The centre segment of poly(ethylene/butylene) is a rubbery segment. The sample characteristics (component weight ratios, total molecular weights and molecular

* To whom correspondence should be addressed. Present address: Du Pont Kabushiki Kaisha, AMAL, 2-2-1 Hayabuchi, Tsuzuki-ku, Yokohama 224, Japan
† Permanent address: Electrotechnical Laboratory, Tsukuba, Ibaraki 305, Japan
‡ We have used the bulk data of polybutadiene for that of poly(ethylene/butylene) in this report since there are no reports on poly(ethylene/butylene) in the literature

Table 1 SEBS sample characteristics

Polymer	Component weight ratio	M_w	M_w/M_n
SEBS (10/80/10)	10/80/10	61 000	1.3
SEBS (15/70/15)	15/70/15	55 000	1.3
SEBS (20/60/20)	20/60/20	61 000	1.3

M_w: weight-average molecular weight. M_n: number-average molecular weight

weight distributions) are listed in *Table 1*. The SEBS films were prepared by dissolving each SEBS in toluene with a concentration of 2% by weight and then spin-coating on freshly cleaved mica substrates (atomically smooth surfaces) at 2000 rpm after filtering the solution through a Millipore Teflon filter (0.2 μm). The films were annealed at 100°C for 72 h under vacuum (0.5 torr) and cooled down to room temperature. The film thickness thus obtained was about 170 nm.

The AFM topography images were obtained in the constant repulsive force mode by an AFM (SPA-300, Seiko Instruments Inc., Japan) with a V-shaped micro-fabricated cantilever (Olympus Opt. Inc., Japan) with a length of 100 μm, Si_3N_4 pyramidal tip (apex radius $\simeq$ 20 nm), and a spring constant of 0.1 N m^{-1}. In the normal repulsive force mode, the surface was seriously damaged during tip scanning, which became more severe with the increase of poly(ethylene/butylene) content in the SEBS samples. This is because the strong attractive interaction between the tip and the sample (adhesion force and water meniscus force[21]) deformed the soft SEBS samples. Therefore, for the AFM measurement described in this report, the tip was positioned at just before the pull-off position, as indicated by an arrow in *Figure 1*. This AFM tip position is still in the repulsive force region but very weak, so that the tip effect is minimized.

RESULTS AND DISCUSSION

Figures 2a–c are AFM topographic images of the three types of SEBS film. The characteristic morphologies

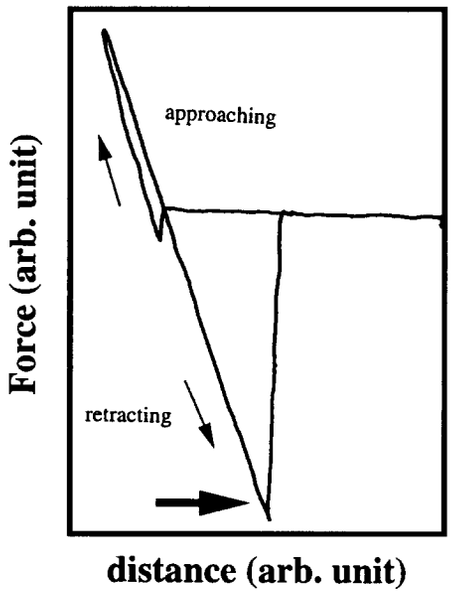

Figure 1 Representative data of approaching and retracting force vs distance curve. The AFM tip was positioned at a point marked by an arrow

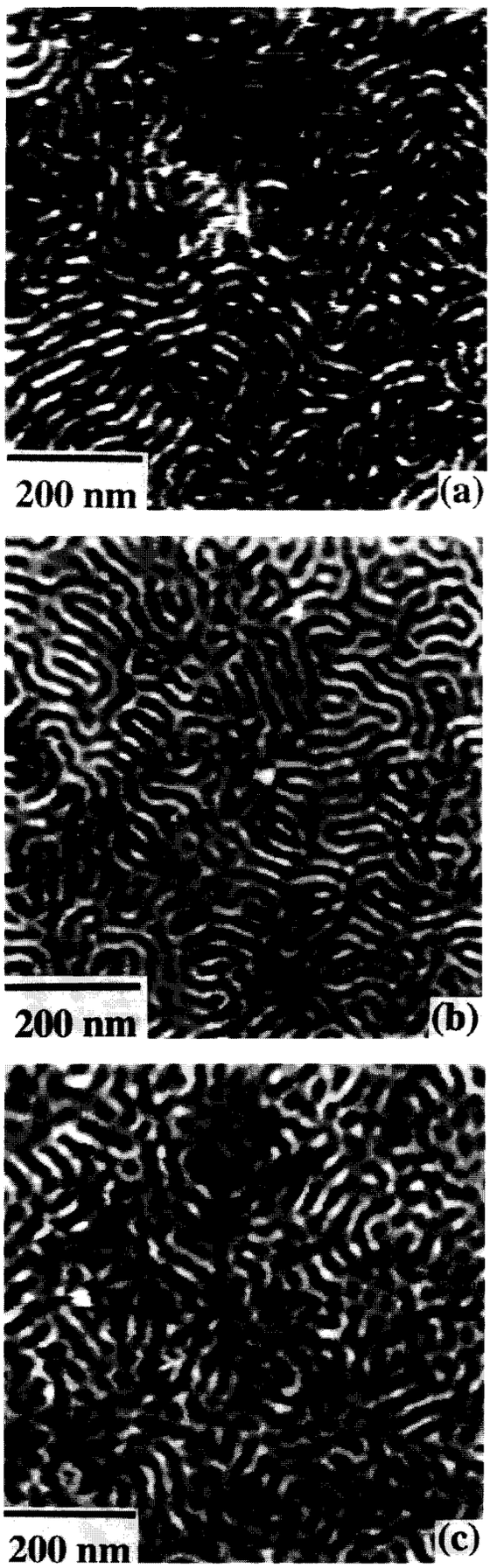

Figure 2 AFM topographic images of thin films of (a) SEBS (10/80/10), (b) SEBS (15/70/15) and (c) SEBS (20/60/20). The maximum grey scales for the height are 13, 16 and 20 nm, respectively

consisting of hills and valleys were obtained. With increasing ratio of the polystyrene component, the hills are likely to grow from long worm-like to mesh-like microphase domains. Such a topographic difference will be caused by the difference of the free surface energies between polystyrene and poly(ethylene/butylene). In order to see this effect clearly, we calculated the fraction of the hills in these images as 39.9, 55.9, and 65.6%, respectively. This increase of the hills with polystyrene content indicates that the hills correspond to polystyrene and the valleys to poly(ethylene/butylene). The result of two different domains consisting of polystyrene and poly(ethylene/butylene) is very similar to that of thin films of polystyrene and poly(methyl methacrylate) blend systems reported by Tanaka *et al.*[22]. They observed that polystyrene with lower surface energy covers the topmost surface on the thick film (25 μm) systems, whereas two domains consisting of each polymer appear on the surfaces on the thin film ($\sim$100 nm) systems. Such specific phenomena for thin film systems have been reported[18,23]. The similar effect of thick films for block copolymers has been also observed by TEM[24]; however, there is still a possibility that we observed the inner structure just under the thin covering layer[24,25] of poly(ethylene/butylene) with lower surface energy[26] since AFM data do not provide any information on the surface component. The origin of the hill structure of polystyrene, which has higher surface energy than poly(ethylene/butylene)[26], is also interpreted by using Tanaka's model[22] which explains the hill formation of the material with higher surface energy.

Here, we compare the results of the surface morphologies obtained by AFM with the bulk morphologies. Bulk morphology of triblock copolymers is mainly governed by the volume ratio of the phases. The TEM study has revealed that spheres of a minor component can be formed in a continuous major matrix at a volume fraction of about $\leq$25% for the minor component[3]. In our SEBS samples, the volume fractions of polystyrene are found to be about 17, 27 and 36%, respectively, using typical density data[26] of 1.05 for polystyrene and 0.89 for poly(ethylene/butylene). If surface morphologies are similar to the bulk morphologies, the AFM morphology should be a spherical structure of polystyrene for SEBS (10/80/10), a rod-like structure or an intermediate between spherical and lamellar structure of polystyrene for SEBS (15/70/15), and lamellar structure for SEBS (20/60/20)[3]. However, our AFM results contradict the above conjecture. The AFM images in *Figure 2a–c* show that the surface morphology resembles a rod-like structure or an intermediate between spherical and lamellar structure of polystyrene for SEBS (10/80/10), a bicontinuous or lamellar structure for SEBS (15/70/15), and a spherical or rod-like structure of the major component of poly(ethylene/butylene) for SEBS (20/60/20). Thus the surface morphologies of our AFM results, which are completely different from the bulk morphologies, will be caused by the effect of the surface segregation of polystyrene.

Figure 3 represents cross-sectional profiles for the three SEBS samples, showing the height difference between hills and valleys and the periodicity distance. The height difference increased with polystyrene content. Averaging over the various positions of several micrographs, we found the height difference in each image was

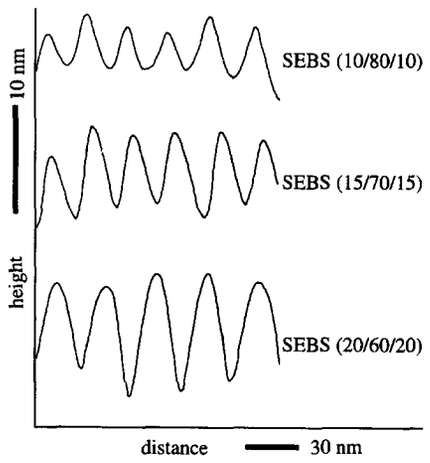

Figure 3 Representative cross-sectional profiles of SEBS (10/80/10), SEBS (15/70/15) and SEBS (20/60/20). The height scale is extremely expanded compared with the distance scale

Table 2 Comparison of the periodicity distance (d), measured by AFM and predicted

Sample	d (AFM)	d (prediction)
SEBS (10/80/10)	29.5 $\pm$ 0.8 nm	26 nm
SEBS (15/70/15)	30.8 $\pm$ 1.1 nm	26–28 nm
SEBS (20/60/20)	33.9 $\pm$ 0.9 nm	25–27 nm

calculated as 3.9 $\pm$ 0.3, 8.2 $\pm$ 0.4 and 11.3 $\pm$ 1.0 nm, respectively. This increase in height difference with polystyrene component can be explained by the increase of the repulsive forces[27] between polystyrene and poly(ethylene/butylene). The specific values of periodicity distance in each image were obtained as 29.5 $\pm$ 0.8, 30.8 $\pm$ 1.1 and 33.9 $\pm$ 0.9 nm, respectively (*Table 2*). The slight increase of periodicity distance with polystyrene content was also obtained by SAXS[28]. As for the theoretical predictions, Helfand and Wasserman[29,30] calculated the periodicity distance in bulk triblock copolymers (*Table 2*) and confirmed its accuracy by comparing it with many experimental data obtained by TEM or SAXS. Both results (*Table 2*) are in reasonable agreement, indicating that the periodicity distance of the surface and that of the bulk are almost the same.

Figure 4 shows typical force vs distance curves on the hills and valleys of SEBS (15/70/15) using the same AFM tip. Both curves show hysteresis between the approaching and retracting curves, due to the adhesion force. It is larger on the valleys than on the hills. We measured these force vs distance curves on each domain surface to estimate the local stiffness. The slope for the valleys is less steep than that for the hills, indicating that the valleys are softer than the hills. We can thus confirm that the hills correspond to polystyrene and the valleys to rubbery poly(ethylene/butylene). In addition, by fitting the force vs distance curves in *Figure 3* to a Herzian model[31], we can estimate the local Young's modulus of each domain on the assumption that the AFM tip apex is a rigid sphere, using the following equation[32,33]:

$$F(h) = k_c[h - F(h)^{2/3}(D^2/R)^{1/3}] \quad (1)$$

Here $F(h)$ is the applied force on the sample as a result of the cantilever deflection as a function of the movement of the piezo scanner stage of h, k_c the spring constant of the

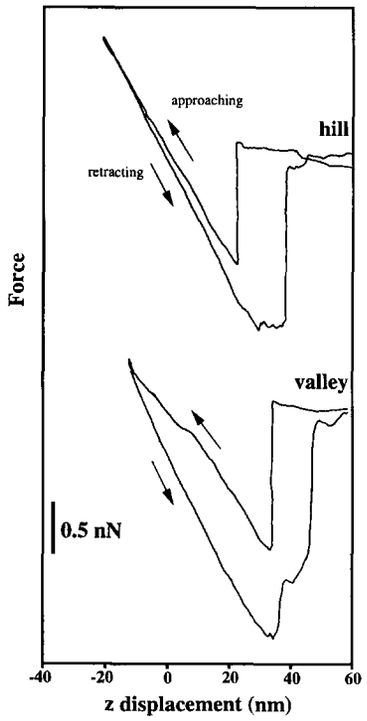

Figure 4 Force vs distance curves on the hills and valleys measured using the same AFM tip with a spring constant of $0.1\,N\,m^{-1}$. The approaching and retracting speed of the cantilever was $4\,nm\,s^{-1}$

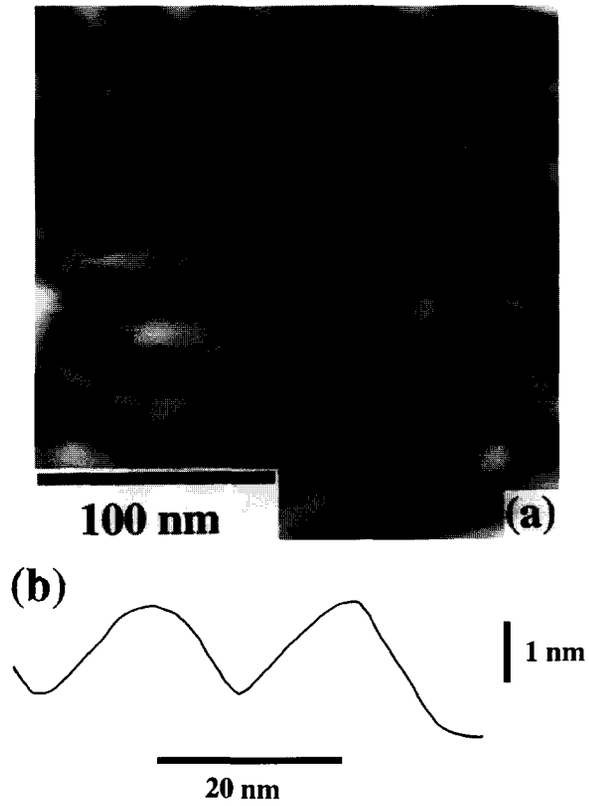

Figure 5 (a) High magnification AFM image of SEBS (15/70/15) showing height modulation on the hills. The maximum grey scale for the height is 13 nm. A cross-sectional profile (b) of the hill part shown in (a) exhibits the modulated structure with a height of about 2 nm and a periodicity of about 20 nm

cantilever, R the radius of the tip apex, and D is related to Young's modulus E and Poisson's ratio σ in the form of $D = 3(1-\sigma^2)/4E$. The values of these parameters are given in *Table 3*. The local Young's moduli were calculated as 24 ± 3.1 MPa for polystyrene and 6.4 ± 0.3 MPa for poly(ethylene/butylene)§. Our result for polystyrene obtained using equation (1) is much lower than that of the bulk as generally reported**. This may be due to the effect of the soft poly(ethylene/butylene) surrounding and supporting the polystyrene underneath since the periodicity distance is as small as 30 nm, which is close to the size of the AFM tip radius. Other possibilities are that there still exist some uncertain factors such as the contact area, tip radius and geometry, and the local value of Poisson's ratio.

The higher magnification AFM topographic image of SEBS (15/70/15) is shown in *Figure 5a* and the cross-sectional profile along the line marked in *a* is given in *Figure 5b*. The height modulation of ~2 nm is clearly seen on the polystyrene parts with a periodicity of 20–30 nm. Similar structures were observed on SEBS (20/60/20), but we could not clearly detect such structures on SEBS (10/80/10) since the softness of this copolymer made it difficult to image the higher magnification. This is because SEBS (10/80/10) contains a large quantity of soft and rubbery poly(ethylene/butylene). In the cases of SEBS (15/70/15) and SEBS (20/60/20), however, we expect that polystyrene spontaneously formed some uniform structure leading to a moniliform structure during annealing. In order to confirm this, we observed

Table 3 Estimated local Young's modulus of polystyrene and poly(ethylene/butylene)

Domain	Poisson's ratio	Estimated local Young's modulus (MPa)
Polystyrene	0.33	24 ± 3.1
Poly(ethylene/butylene)	0.49	6.4 ± 0.3

the morphological change at the early phase-separation stage. *Figures 6a–c* show AFM topographic images of SEBS (15/70/15) without annealing, annealed at 100°C for 30 min and at 100°C for 150 min under vacuum (0.5 torr), respectively. Without annealing, the surface morphology showed many granules, and then, with increasing annealing temperature and time, they grew to a worm-like structure by linking to each other on the surfaces. Finally, the surface morphology changed to a bicontinuous structure as shown in *Figure 2b*. In addition, we observed the stability of the polystyrene structures by applying large forces to SEBS surfaces. *Figure 7a* shows a typical AFM topographic image of SEBS (20/60/20) obtained after scanning with large repulsive forces of 15 nN (the central area). Although the surface is seriously damaged due to the AFM tip scanning, we can observe a stable microstructure on such damaged surfaces, as shown in *Figure 7b*. The small structures, 20–30 nm in size, are still observed, as indicated by arrows, even after deformation by the AFM tip. We conclude that polystyrene will spontaneously aggregate during annealing to form such stable structures. We can then propose a model for the surface

§ The deduced Young's moduli have a weak dependence on Poisson's ratio. In our case, we assume that polystyrene and rubbery poly(ethylene/butadiene) have Poisson's ratios of 0.33 and 0.49 respectively (ref. 1, p. 7)

** For example, the bulk Young's modulus of polystyrene is 3.4 GPa in the literature (ref. 1, p. 7)

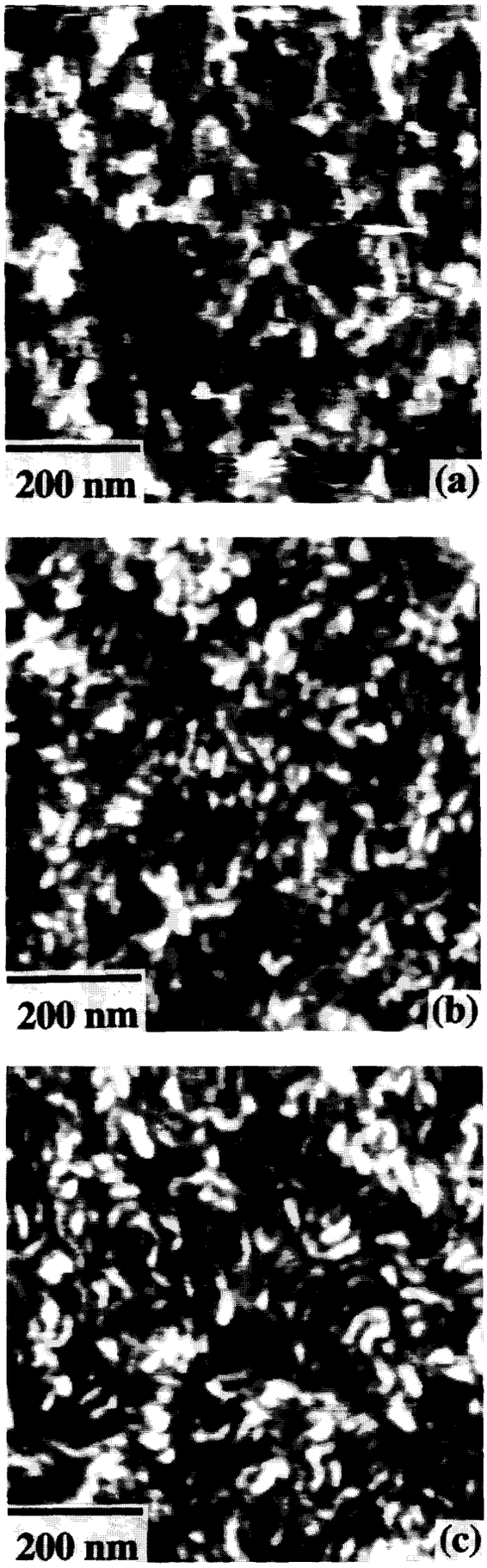

Figure 6 AFM topographic image of SEBS (15/70/15) surface: (a) without annealing; (b) annealed at 100°C for 30 min; and (c) at 100°C for 150 min under vacuum (0.5 torr)

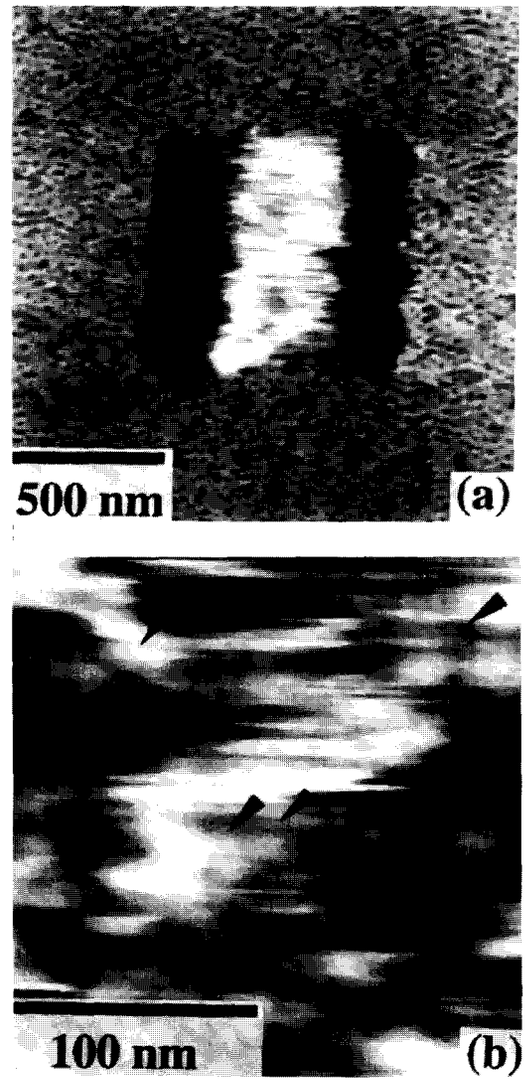

Figure 7 (a) AFM topographic image of SEBS (20/60/20) after large force scanning (central area of 850 × 850 nm^2) of 15 nN with the AFM tip. Higher magnification AFM images (200 × 200 nm^2) (b) of the central area in (a). Typical self-aggregated and stable structures of polystyrene are indicated by arrows in (b)

structures of SEBS. *Figures 8a* and *b* show schematic drawings of cross-sectional and top views of the surface structure of SEBS, respectively. Polystyrene (hard segment) aggregates together and forms hills like islands in a poly(ethylene/butylene) (rubbery segment) sea. In addition, the polystyrene parts show stable moniliform structures with a small height modulation of 1–2 nm on the topmost surface. This may result from the linkage of granular polystyrene and the minimization effect of the surface area or energies.

We estimate how many polystyrene blocks in terms of SEBS (15/70/15) and SEBS (20/60/20) molecules are required for the stable structures. Here, to simplify the calculation, we assume the shape of one unit of the moniliform polystyrene parts (*Figure 8*) to be a column (the radius is half the width of the polystyrene parts and the height is the periodic undulation distance). The number of polystyrene blocks (N) forming one unit is estimated by the following equation:

$$N = \rho AV/M \qquad (2)$$

Here ρ is the density of polystyrene, A Avogadro's number, V the volume of the column, and M the

Table 4 Calculated number of polystyrene blocks (N); d = diameter, h = height of the column obtained by AFM, V = volume of the column and M = molecular weight of a single polystyrene block

Sample	d (nm)	h (nm)	V (nm^3)	M	N
SEBS (15/70/15)	16.6	20–30	6000–9000	8250	310–470
SEBS (20/60/20)	19.5	20–30	4300–6500	12200	310–480

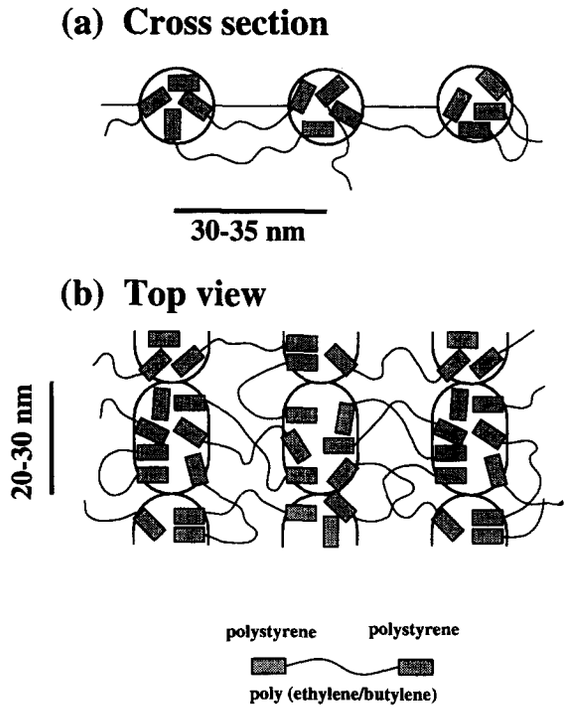

Figure 8 Schematic drawings of the surface structure of SEBS films showing the formation of the self-organized structure of polystyrene: (a) top view, and (b) cross-sectional view. The hard segment of polystyrene is presented as rectangular blocks and the rubbery segment of poly(ethylene/butylene) as strings

molecular weight of the polystyrene block in SEBS (15/70/15) or SEBS (20/60/20) molecules on one side. V and M values for SEBS (15/70/15) and SEBS (20/60/20) were calculated using the average widths of the polystyrene domains (16.6 nm for SEBS (15/70/15) and 19.5 nm for SEBS (20/60/20) as determined directly from *Figures 2b* and *d*, respectively), the repeat distance of the undulation (20–30 nm for both SEBS (15/70/15) and SEBS (20/70/20)), the component weight ratios and the total molecular weights. With $\rho = 1.05$ (ref. 26), $A = 6.02 \times 10^{23}$, $V = 6000$–9000 and $M = 8250$ for SEBS (15/50/15), and $V = 4300$–6500 and $M = 12200$ for SEBS (20/60/20), the number of polystyrene blocks forming one unit is found to be 310–480 for SEBS (15/70/15) and 310–470 for SEBS (20/60/20). The details are summarized in *Table 4*. These two values are quite similar, indicating the presence of some specific aggregation number for the polystyrene blocks.

CONCLUSION

We have demonstrated not only the visible mapping of the microphase domains composed of polystyrene and poly(ethylene/butylene) of SEBS triblock copolymer surfaces but have also differentiated individual polymers on a nanometre scale using AFM techniques. The domain sizes and periodicity distances observed on the surfaces were in agreement with those of theoretical prediction in the bulk. The surface area fraction of the polystyrene parts increased by 39.9, 55.9 and 65.9% with increasing polystyrene content in the block copolymers of 20, 30 and 40 wt%, respectively. The estimated local Young's modulus was about 24 ± 3.1 MPa for polystyrene and 6.3 ± 0.3 MPa for poly(ethylene/butylene); these figures are uncertain in quantity but are qualitatively in agreement with the bulk elastic properties. AFM was also used to confirm the stability of polystyrene domains by applying large forces. We found that the polystyrene parts form a moniliform structure during annealing via a self-assembly-like process, with a height modulation of 1–2 nm. One unit of the stable polystyrene structure is estimated to be composed of 300–500 polystyrene blocks in SEBS molecules.

ACKNOWLEDGEMENT

This work was partly supported by the New Energy and Industrial Technology Development Organization (NEDO).

REFERENCES

1 Nielsen, L. E. 'Mechanical Properties of Polymers', Reinhold Publishing Corp., New York, 1967
2 Carraher, C. E. Jr. and Tsuda, M. 'Modification of Polymer', American Chemical Society, Washington, DC, 1980
3 Noshay, A. and McGrath, J. E. 'Block Copolymers Overview and Critical Survey', Academic Press, New York, 1970
4 Han, C. D., Kim, J. and Kim, J. K. *Macromolecules* 1989, **22**, 383
5 Sawyer, L. C. and Grubb, D. T. 'Polymer Microscopy', Chapman and Hall, New York, 1987
6 Meier, H. and Strobl, G. R. *Macromolecules* 1987, **20**, 649
7 Nojima, S. and Roe, R. J. *Macromolecules* 1987, **20**, 1866
8 Binnig, G., Quate, C. F. and Gerber, C. *Phys. Rev. Lett.* 1986, **56**, 930
9 Grim, P. C. M., Brouwer, H. J., Seyger, R. M., Oostergetel, G. T., Bergsma-Schutter, W. G., Arnberg, A. C., Güthner, P., Dransfeld, K. and Hadziioannou, G. *Makromol. Chem. Macromol. Symp.* 1992, **62**, 141
10 Annis, B. K., Noid, D. W., Sumpter, B. G., Reffner, J. R. and Wunderlich, B. *Makromol. Chem. Rapid Commun.* 1992, **13**, 169
11 Maaloum, M., Ausserre, D., Chatenay, D. and Gallot, Y. *Phys. Rev. Lett.* 1993, **70**, 2577
12 van den Berg, R., de Groot, H., van Dijk, M. A. and Denley, D. R. *Polymer* 1994, **35**, 5778
13 Tsukruk, V. V. and Reneker, D. H. *Polymer* 1995, **36**, 1791
14 Motomatsu, M., Nie, H.-Y., Mizutani, W. and Tokumoto, H. *Polymer* 1996, **37**, 183
15 van Dijk, M. A. and van den Berg, R. *Macromolecules* 1995, **28**, 6773
16 Mate, C. M., McClelland, G. M., Erlandsson, R. and Chiang, S. *Phys. Rev. Lett.* 1987, **59**, 1942
17 Maivald, P., Butt, H. J., Gould, S. A. C., Prater, C. B., Drake, B., Gurley, J. A., Elings, V. B. and Hansma, P. K. *Nanotechnology* 1991, **2**, 103
18 Motomatsu, M., Nie, H.-Y., Mizutani, W. and Tokumoto, H. *Jpn. J. Appl. Phys.* 1994, **33**, 3775
19 Reifer, D., Windeit, R., Kumpf, R. J., Karbach, A. and Fuchs, H. *Thin Solid Films* 1995, **264**, 148
20 Motomatsu, M., Nie, H.-Y., Mizutani, W. and Tokumoto, H. *Thin Solid Films* 1996, **273**, 304
21 Burnham, N. A. and Colton, R. J. *J. Vac. Sci. Technol.* 1991, **A9**, 2548
22 Tanaka, K., Takahara, A. and Kajiyama, T. *Macromolecules* 1996, **29**, 3232

23 Kraush, G., Hipp, M., Böltau, M., Marti, O. and Mlynek, J. *Macromolecules* 1995, **28**, 260
24 Hasegawa, H. and Hashimoto, T. *Polymer* 1992, **33**, 475
25 Grim, P. C. M., Nyrkova, I. A., Semenov, A. N., ten Brinke, G. and Hadziioannou, G. *Macromolecules* 1995, **28**, 7501
26 Brandrup, J. and Immergut, E. H. 'Polymer Handbook', 3rd Edition, Wiley-Interscience, New York, 1989
27 Bates, F. S. and Hartney, M. A. *Macromolecules* 1985, **18**, 2478
28 McIntyre, D. and Campos-Lopez, E. in 'Block Polymers' (Ed. S. L. Aggarwal), Plenum Press, New York, 1970, p. 19
29 Helfand, E. and Wasserman, Z. R. *Macromolecules* 1976, **9**, 879
30 Helfand, E. and Wasserman, Z. R. *Macromolecules* 1978, **11**, 960
31 Landau, L. D. and Lifshitz, E. M. 'Theory of Elasticity', Pergamon, London, 1959, p. 30
32 Nie, H.-Y., Motomatsu, M., Mizutani, W. and Tokumoto, H. *J. Vac. Sci. Technol.* 1995, **B13**, 1163
33 Nie, H.-Y., Motomatsu, M., Mizutani, W. and Tokumoto, H. *Thin Solid Films* 1996, **273**, 143